Available online at www.sciencedirect.com
SCIENCE DIRECT®
Physica D 179 (2003) 1–17
PHYSICA D
www.elsevier.com/locate/physd

Influence of damping on the delta-kicked harmonic oscillator with Heaviside kick

Robert F. Mudde*, Sander G. Jansz

Kramers Laboratorium voor Fysische Technologie, Delft University of Technology, Pr. Bernhardlaan 6, 2628 BW Delft, The Netherlands

Received 4 September 2002; received in revised form 20 November 2002; accepted 24 December 2002
Communicated by Y. Kuramoto

Abstract

A damped harmonic oscillator, kicked at a fixed frequency by a kick with a fixed strength but with a sign given by the sign of the velocity of the oscillator, is investigated. This system is encountered when investigating a water-filled U-tube in which bubbles are released at the bottom. A mapping similar to the one of Scott et al. [Physica D 155 (2001) 34] is used to describe the kicked oscillator, but here incorporating the effect of friction. Similar to Scott et al. [Physica D 155 (2001) 34] the stable orbits can be calculated, but now for the dampened case. The behavior of the oscillator is investigated numerically as a function of its period number and the strength of the friction parameter. In general, the higher the damping the simpler the trajectory of the oscillator and the quicker the steady state is reached. However, for certain values of the period number and the friction parameter complex trajectories are found, some of which may not have reached a steady state, due to slow relaxation. The oscillator responds sensitive to changes in both the period number and the friction parameter. Finally, the influence of the initial conditions on the final mode of the oscillator has been investigated. It is found that the system is sensitive to the initial conditions. In the initial conditions plain, four spiraling arms are found where the mode of the oscillator deviates from the rest of the plain.

PACS: 05.45.+b; 47.55.Kf

Keywords: Nonlinear dynamics; Heaviside kicked harmonic oscillator; Friction; U-tube oscillation

1. Introduction

Kicked oscillators have been used extensively for the study of the transition to chaos. One of the advantages of the kicked oscillator is that they are nonlinear one-dimensional systems. Well known examples are the delta-kicked rotor, the conservative Duffing oscillator and a driven particle in an infinite square well potential (see [11]). The delta-kicked rotor is directly related to the Standard Map. The kicks, that the rotor experiences, have a strength that is the product of a fixed maximum value (or amplitude) K and the cosine of the angular position of the rotor. Klappauf et al. [6] used the concept of the kicked rotor to investigate the quantum chaos in the motion of a Cesium atom in a dipole potential. Many physical systems, both classical and quantum mechanical, can be represented by

* Corresponding author. Tel.: +31-15-278-2834; fax: +31-15-278-2838.
E-mail address: r.f.mudde@klft.tn.tudelft.nl (R.F. Mudde).

0167-2789/03/$ – see front matter © 2003 Elsevier Science B.V. All rights reserved.
doi:10.1016/S0167-2789(03)00006-X

a delta-kicked oscillator. For instance, Tanabe et al. [15] considered a kicked harmonic oscillator that represents a train of electric pulses 'hitting' an atom. Their interaction potential is a series of delta functions of time, where the strength of the kick is a fixed momentum transfer multiplied by the distance from the oscillating particle to the origin. This means that the kick has a fixed sign, but a variable strength. Gardiner et al. [5] investigated quantum chaos in an ion trap, representing the system by a delta-kicked harmonic oscillator. In their case, the kick has a strength proportional to the cosine of the position of the oscillator like in the case of the kicked rotor. However, their unkicked part of the Hamiltonian is that of a harmonic oscillator. Furthermore, their system is a quantum mechanical one. Chernikov et al. [3], as well as Afanasiev et al. [1] considered a kicked harmonic oscillator that represents a charged particle moving in a constant magnetic field and in an electric field of wave packed type. This results in kicks that depend on the sinus of the position of the particle. The same system was investigated by Lichtenberg and Wood [7]. Scott et al. [12] investigated a single ion trapped in a harmonic potential. The ion is subjected to delta-kicks due to a periodic sequence of laser pulses, the strength of the kicks varying via a Gaussian due to the Gaussian structure of the laser. The analysis performed was both in terms of a classical and a quantum mapping.

It has been shown by Zaslavskiĭ et al. [18] that systems with only one and a half degree of freedom can show stochastic diffusion. They considered a particle in a magnetic field kicked by electric wave packages, i.e. the same system as [3,7], and showed that for resonance conditions in the phase plane a regular separatrix mesh is formed. Inside this mesh the phase trajectories are closed curves, whereas on the mesh the particle follows a random walk. The mesh was called a stochastic web. In [17] dissipation in the same system is taken into account. The dissipation is introduced into the equation of motion of the particle as being proportional to the particle velocity. It was found that the dissipation restricts the stochastic acceleration of the particle and strange attractors are observed. The strange attractors are explained by the trapping of the particle by the wave. The trapped particle reaches a position where the coupling with the magnetic field becomes so strong that the particle is kicked out of the trap and via the damped harmonic motion spirals back to the origin where it is trapped in another wave.

All the above cited papers have in common that the strength of the kicks is 'sampled' by the system from a continuous function and can thus have any value from $\{-K, K\}$ or $\{0, K\}$. In recent work of Scott and Milburn [14] and Scott et al. [13], kicked oscillators were investigated that resemble circle packings. The oscillators were described by a Hamiltonian of the type [13]

$$\mathcal{H}(x, p, t) = \frac{1}{2}\omega(x^2 + p^2) + K|x| \sum \delta_{\mathrm{D}}(t - n). \tag{1}$$

As is clear from the Hamiltonian, the kicks have a fixed strength, K, but a variable sign. The latter is determined from the sign of the position, x, of the oscillator. The action of the kicks on the oscillator is to change instantly the momentum of the oscillator by a finite amount, $-K\,\mathrm{sgn}(x)$, leaving the position of the oscillator unchanged.

In the present work we encountered a damped harmonic oscillator that is periodically delta-kicked with a kick that has a binary strength: the kick is either K or $-K$, depending on whether the velocity of the oscillator is negative or positive, respectively. Besides, the kick does not affect the momentum of the oscillator but instead the out of equilibrium position of the oscillator is changed instantaneously by the kick. The system under consideration is a simple U-tube filled with water. Periodically, bubbles are fed to the bottom of the U-tube. This is a system that obviously belongs to the area of classical mechanics. The kicked U-tube has previously been investigated by Beek and Van Den Berg [16], who studied the system in the context of interplaying time scales. Furthermore, they performed some experiments on an U-tube filled with water and kicked by air bubbles. In the present work the mathematical formulation of the kicked U-tube deviates slightly from that of Beek and Van Den Berg making the undamped version of the kicked U-tube similar to the oscillator of Scott et al. [13]. However, the damping due to friction is an important aspect of the present work.

The motivation of the present work is the occurrence of so-called vortical structures in gravity driven bubble flows (see e.g. [8–10]), which are caused by the interplay between density differences (i.e. non-uniformities in spatial bubble distribution), gravity and fluid flow. In this context the U-tube is an abstraction of the complicated interplay seen in the bubbly flows.

2. Theoretical description

Consider a U-tube as shown in Fig. 1. The U-tube is filled with water up to a height h_0. In the description of the U-tube oscillations we will ignore the width of the U. This means that the total length of the water is equal to twice the water level height: $L = 2h_0$. At the bottom of the U-tube, bubbles are injected one by one at a fixed frequency f_b. Each injected bubble moves into either the left leg or the right leg. As we assume that the width of the U-tube is 0, each bubble will instantaneously be either in the left or in the right leg. The choice of this is dictated by the direction of the velocity of the water in the tube at the moment the bubble is introduced: if the water moves from the left to the right leg, the bubble will go the right leg (and the other way around).

The bubbles will set the water in the U-tube in motion and induce an oscillation. This oscillation in turn influences the direction of the next entering bubble. The oscillation of the U-tube can be described easiest in terms of the 'out of equilibrium' position of the water level in leg 2, defined as

$$\delta \equiv \delta_2 = h_2 - h_{2,\mathrm{eq}}. \tag{2}$$

Note that in the above equation, the equilibrium height in leg 2 is not denoted by h_0. The reason is, that when a bubble is present in, e.g. leg 2 the equilibrium height is not necessarily equal to this height h_0. For small amplitudes of the oscillation, the liquid flow in the U-tube will be laminar, consequently a damping term linear in the liquid velocity, hence proportional to $\dot{\delta}$, will be present. The liquid oscillation, in terms of δ is described by

$$\ddot{\delta} + \tilde{\mu}\dot{\delta} + \frac{2g}{L}\delta = 0 \tag{3}$$

with $\tilde{\mu}$ representing the friction coefficient, g the acceleration due to gravity and L twice the water height (without bubbles). Obviously, the frequency of the oscillator in case of zero friction is $\sqrt{2g/L}$. It is convenient to use a dimensionless time: $\tau = \sqrt{2g/L}t$. The oscillator is then described by

$$\ddot{\delta} + 2\mu\dot{\delta} + \delta = 0 \tag{4}$$

with solution given by

$$\delta(\tau) = \mathrm{e}^{-\mu\tau}\left(A\sin\sqrt{1-\mu^2}\tau + B\cos\sqrt{1-\mu^2}\tau\right). \tag{5}$$

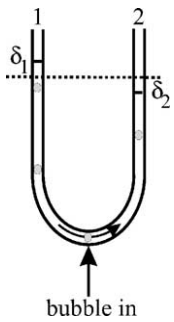

Fig. 1. Geometry of the oscillating U-tube.

2.1. Bubble events

The bubbles one by one enter the U-tube at its lowest point at regular times nT_b, i.e. at dimensionless times $n\phi$ with $\phi = T_b/T_0$, T_0 being the oscillation period of the frictionless U-tube. When a bubble enters the U-tube a series of events is started that influence the oscillation of the U-tube.

2.1.1. Bubble entering

When a bubble enters the U-tube, the levels in both legs rise by an amount $(1/2)V_b/A$, V_b is the bubble volume, A denotes the cross-sectional area of each of the legs. Obviously, this bubble event does not change the motion of the U-tube, as is easily seen by calculating the change in the out of equilibrium position δ:

$$h_i^{\text{new}} = h_i^{\text{old}} + \frac{1}{2}\frac{V_b}{A}, \qquad h_i^{\text{new,eq}} = h_i^{\text{old,eq}} + \frac{1}{2}\frac{V_b}{A} \tag{6}$$

with h_i^{new}, h_i^{old}, $h_i^{\text{new,eq}}$, $h_i^{\text{old,eq}}$ the water level in leg $i = 1, 2$ after the bubble event, before the bubble event, the equilibrium level after the bubble event and before, respectively. The out of equilibrium position δ is thus according to Eq. (2) unchanged when a new bubble enters the U-tube.

2.1.2. Bubble chooses leg

Next, the introduced bubble chooses one of the legs, depending on the direction of the liquid velocity at the inlet point. The height of the liquid level is unchanged by this choice. The equilibrium position, however, does change with again $(1/2)V_b/A$, but whether this is added or subtracted depends on the choice of the leg. If the bubble chooses leg 1, the equilibrium level in leg 1 increases with $(1/2)V_b/A$ and decreases with $(1/2)V_b/A$ in leg 2. The choice of the bubble is completely determined by the sign of the liquid velocity in the U-tube. If the velocity is positive, the bubble will enter leg 2 (according to the definition for δ). Hence, we find for the changes in height and in equilibrium position:

$$h_i^{\text{new}} = h_i^{\text{old}}, \qquad h_i^{\text{new,eq}} = h_i^{\text{old,eq}} + \frac{1}{2}\frac{V_b}{A}\operatorname{sgn}(\dot{\delta}) \tag{7}$$

with $\operatorname{sgn}(\cdot)$ denoting the sign of the argument. This means that for δ the jump condition is

$$\delta^{\text{new}} = \delta^{\text{old}} - \frac{1}{2}\frac{V_b}{A}\operatorname{sgn}(\dot{\delta}). \tag{8}$$

By definition, a bubble chooses leg 2 if the velocity is 0, hence $\operatorname{sgn}(0) \equiv 1$.

2.1.3. Bubble leaving

If the bubble leaves the system, the level in the leg the bubble is in, drops instantaneously with V_b/A. However, the same holds for the equilibrium level in that leg. The other leg does not change: nor in liquid level height, nor in equilibrium position. So, a bubble leaving the system does not alter δ. Note, that all bubble events do not change $\dot{\delta}$.

2.2. Mathematical formulation

From the above we have that directly after the introduction of a new bubble, the oscillating is kicked. This kick has a fixed kick-strength, denoted by K. Contrary to the kicks mentioned in Section 1, here the kick does not change the momentum of the system, but instead changes instantaneously its position (with respect to the equilibrium position). Mathematically, this can be formulated as

$$\dot{\delta}_{\text{new}} = \dot{\delta}_{\text{old}}, \qquad \delta_{\text{new}} = \delta_{\text{old}} - K\operatorname{sgn}(\dot{\delta})\delta_D(\tau - n\phi) \tag{9}$$

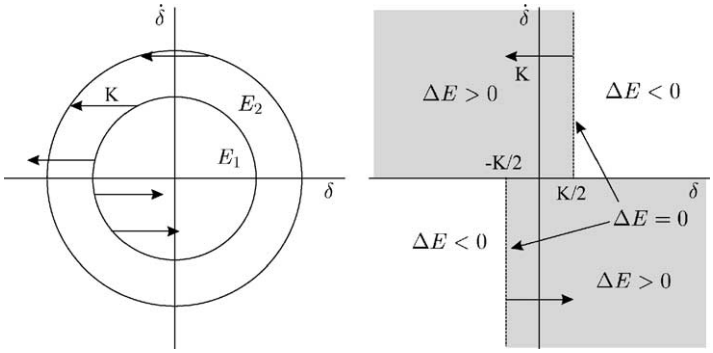

Fig. 2. Phase plot: effect of kicks on the energy.

with $\delta_{\mathrm{D}}(\cdot)$ the delta function of Dirac, τ the dimensionless time and $n\phi$ the discrete dimensionless times at which the oscillator is kicked.

For the undamped case, a Hamiltonian can be formulated:

$$\mathcal{H} = \frac{1}{2}p^2 + \frac{1}{2}\delta^2 - K|p| \sum \delta_{\mathrm{D}}(\tau - n\phi) \tag{10}$$

with p the momentum associated with δ. It is easy to verify that this Hamiltonian leads to the rules for the bubble induced kick given in Eq. (9). Obviously, the Hamiltonian shows great similarities with the one of Eq. (1) used by Scott et al. [13].

The solution of the kicked oscillator is trivial: in between the kicks it is a damped oscillator. At each kick the velocity is unchanged, but the position is. This means that the energy of the system is not conserved. Furthermore, the kicks can both increase or decrease the total energy. This is evident from a phase plot, see Fig. 2, where an example of a phase portrait is plotted for negligible friction.

The kicks have two effects on the trajectory: depending on the position in phase space different amounts of energy are added or subtracted. In general, the closer to the δ axis, the bigger the change in energy. For the points on the lines $\{\delta = K/2, \dot{\delta} > 0\}$ and $\{\delta = -K/2, \dot{\delta} < 0\}$ the energy change is 0. The second effect is that the kicks always put the phase of the oscillation back. Consequently, the oscillation time is increased by the kicks. Here it holds that a kick at a point closer to the $\dot{\delta}$ axis the bigger the jump in the phase. Notice that the phase jump is exactly 0 at $\dot{\delta} = 0$.

3. Periodic orbits

Following the mapping proposed in [13] the mapping from $\{\delta, \dot{\delta}\}$ from just before a kick to one bubble time T_{b} later can be written as the kick followed by a rotation and in the present case a damping due to friction. Due to the damping, the trajectory in phase space is easier described in transformed coordinates $\{u, v\}$:

$$u = \sqrt{1-\mu^2}\delta, \qquad v = \dot{\delta} + \mu\delta. \tag{11}$$

In the new coordinates, obviously the nth kick gives a change in both coordinates:

$$u^n \to u^n - \sqrt{1-\mu^2}Ks^n, \qquad v^n \to v^n - \mu K s^n \tag{12}$$

with s^n denoting $\mathrm{sgn}(\dot{\delta})$ just before the nth kick.

The mapping from just before a kick to one bubble time later can now be written as

$$\begin{pmatrix} u^{n+1} \\ v^{n+1} \end{pmatrix} = \mathrm{e}^{-\mu\phi} \begin{pmatrix} \cos\sqrt{1-\mu^2}\phi & \sin\sqrt{1-\mu^2}\phi \\ -\sin\sqrt{1-\mu^2}\phi & \cos\sqrt{1-\mu^2}\phi \end{pmatrix} \begin{pmatrix} u^n - \sqrt{1-\mu^2}Ks^n \\ v^n - \mu Ks^n \end{pmatrix}. \tag{13}$$

Following [13], the above mapping can be rewritten by introducing $z = u + \mathrm{i}v$:

$$z^{n+1} = \mathrm{e}^{-(\mu+\mathrm{i}\sqrt{1-\mu^2})\phi} \left(z^n - \sqrt{1-\mu^2}Ks^n - \mathrm{i}\mu Ks^n \right). \tag{14}$$

Periodic points, z^0, with period n are found by solving

$$z^0 \equiv z^n = \mathrm{e}^{-n(\mu+\mathrm{i}\sqrt{1-\mu^2})\phi} z^0 - K\left(\sqrt{1-\mu^2} + \mathrm{i}\mu\right) \sum_{k=0}^{n-1} \mathrm{e}^{(k-n)(\mu+\mathrm{i}\sqrt{1-\mu^2})\phi} s^k \tag{15}$$

which gives for z^0

$$z^0 = \frac{K(\sqrt{1-\mu^2} + \mathrm{i}\mu)}{1 - \mathrm{e}^{n(\mu+\mathrm{i}\sqrt{1-\mu^2})\phi}} \sum_{k=0}^{n-1} \mathrm{e}^{k(\mu+\mathrm{i}\sqrt{1-\mu^2})\phi} s^k \tag{16}$$

provided $n(\mu + \mathrm{i}\sqrt{1-\mu^2})\phi \neq 2\pi\mathrm{i}$, which holds for any $\mu \neq 0$. Note that $\{s^k = \pm 1\}$, with by definition $s = 1$ if $\dot{\delta} = 0$. The sequence $\{s^k\}$ uniquely defines the periodic orbit.

The above describes the evolution of the periodic points with increasing friction. However, the stability of a periodic orbit is not known. The understanding of which orbits are legitimate is complicated by the friction. Scott et al. [13] considered the frictionless case and showed that the mapping can then be decomposed into two involutions. Obviously, the friction does not allow for such a decoupling and hence the theorems proven by Scott et al. [13] do not hold. An example of the dependence of the stable point on μ is shown in Fig. 3 for $\phi = 0.76$, $K = 0.1$ and μ ranging from 0 to 0.9.

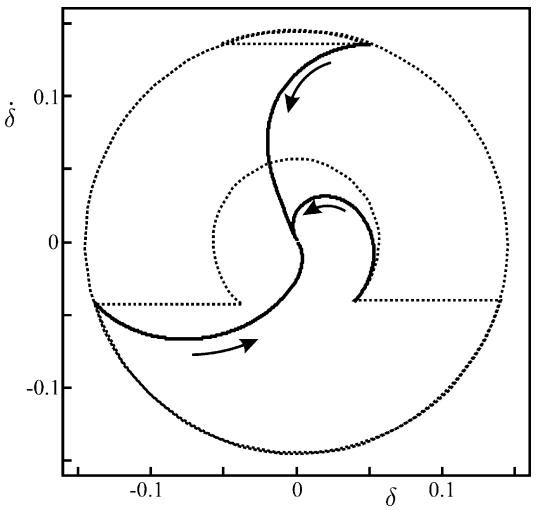

Fig. 3. Behavior of the stable points of period 3 (full lines) for $\phi = 0.76$, $K = 0.1$ and μ ranging from 0 to 0.9. The arrows indicate the direction of increasing μ. The dotted curve is the trajectory in phase space for $\phi = 0.76$, $K = 0.1$, $\mu = 2 \times 10^{-3}$.

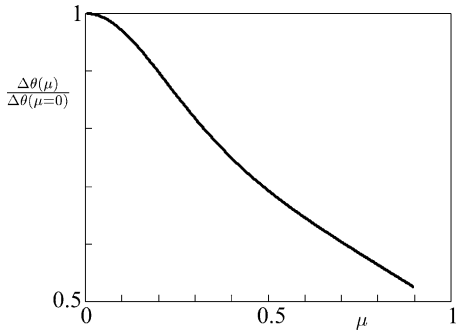

Fig. 4. Dependence of the relative phase change on the friction for $\phi = 0.76$, $K = 0.1$ and the $1/2$ mode.

4. Phase locking, Farey tree and bubble sequences

The kicks induced by the bubbles cause the phase of the oscillation to be set back. In real time, this means that the oscillation period is changed from T_0 to $T_0^{\text{locked}} = T_0(1 - (\Delta\theta/2\pi))$. It is convenient to represent both the unlocked period T_0 and the locked oscillation time T_0^{locked} in terms of the bubble injection period, T_b: $\phi \equiv T_\text{b}/T_0$, called the period number and $\Omega = T_\text{b}/T_0^{\text{locked}}$, which is generally called the rotation number. For zero friction, the phase change is in a simple way related to the period number and the rotation number: $\Delta\theta(\mu = 0) = 2\pi(1 - (\phi/\Omega))$. As the kicks cause the phase to be set back, we again see that Ω will be smaller than or equal to ϕ. The ratio $\Delta\theta(\mu)/\Delta\theta(\mu = 0)$ can for any stationary orbit be calculated from the periodic points. In Fig. 4 this ratio is plotted for $\phi = 0.76$, $K = 0.1$ and the $1/2$ mode (i.e. a sequence $s^k = \{1, -1, 1, -1, \ldots\}$). It is seen that friction causes the phase jump to decrease and thus the oscillation period to be closer to the original period, T_0, of the oscillator.

For a period number of $1/2$ the U-tube is kicked twice per oscillation period. Hence, we can expect that bubbles will alternatively go to leg 1 and leg 2. We will describe this sequence by LRLRLR... (L denoting the leg 2, R the leg 1). When increasing the period number, the rotation number will be unchanged: the systems is locked to 1/2 mode. If the increase is too large, the 1/2 mode becomes unstable and the rotation number jumps to the next mode, which is also a ratio of two integers. The possible rotation numbers are formed like the elements of the Farey tree. This tree starts with two possible states: 0/1 and 1/1. In the terminology of the bubble sequences this would mean LLLL... and RRRR..., respectively. The Farey tree grows according to the following rule:

$$\frac{p_1}{q_1} \oplus \frac{p_2}{q_2} = \frac{p_1 + p_2}{q_1 + q_2}. \tag{17}$$

The first few layers are shown in Fig. 5.

Note that if p/q is an element of the Farey tree, then also $(q - p)/q$ is an element. Obviously, if the first one is smaller than $1/2$ then the second one is larger than $1/2$. Any bubble sequence of the oscillating U-tube can be split into elementary parts, that contain only one switch from L to R. For example, the sequence LLRLLRRLLR can be split into LLR–LLRR–LLR. A sequence of length n with only one switch is coupled to $1/n$ or $(n - 1)/n$, e.g. LLLRRR is $1/6$ or $5/6$. So, the three elements of the example are coupled as: LLR $\leftrightarrow$ $1/3$ and LLRR $\leftrightarrow$ $1/4$. Thus, the sequence itself couples to: LLRLLRRLLR $\leftrightarrow$ $1/3 \oplus 1/4 \oplus 1/3 = 3/10$.

4.1. Example

The kicked oscillator is set at a period number of $\phi = 0.76$, a damping parameter $\mu = 3 \times 10^{-5}$ and a kick strength of $K = 0.1$. The oscillator is started with initial conditions $\delta(0) = 0$ and $\dot{\delta}(0) = 0$. After kicking by 1×10^6

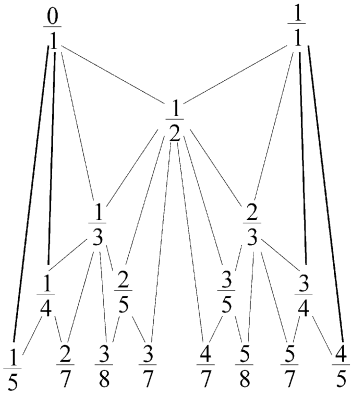

Fig. 5. Farey tree.

bubbles the trajectory in phase space is recorded for another 2000 kicks. The phase portrait is shown in Fig. 6. As is seen, the system locks to an LLR-sequence, with rotation number 2/3.

The trajectory in phase space is a closed curve; the oscillator is in a periodic motion with exactly three kicks in two rotations in phase space in agreement with the rotation number. The trajectory shows a jump from the outer orbit at point A to B on the inner orbit. From point B to C the inner orbit is followed during a time ϕ after which the kick puts the trajectory back on the outer orbit. From D to E the trajectory follows the outer orbit. The kick at E is exactly such that F is also on the outer orbit, on which then the trajectory continues to point A, completing the cycle. As is seen from the plot, the trajectory is a symmetric figure. The points {A,C,E} are stable points with period 3. Their coordinates in phase space follow from Eq. (16) by inserting the sequence $\{s^k\} = \{1, 1, -1\}$ and its permutations. From the coordinates, the phase jumps can be calculated. As the figure is almost symmetric, the total phase jump in one revolution is $\Delta\theta = 1/2(2\Delta\theta_1 + \Delta\theta_2)$, with $\Delta\theta_1 = -0.5276$, $\Delta\theta_2 = -0.7043$ and thus $\Delta\theta = -0.8797$. On the other hand, $\Delta\theta = 2\pi(1 - (\phi/\Omega))$, which by inserting $\phi = 0.76$ and $\Omega = 2/3$ gives indeed almost the same value as it should for this small value of μ. It is observed that most orbits exhibit a large degree of symmetry, especially those with a rotation number that is the ratio of two small integers.

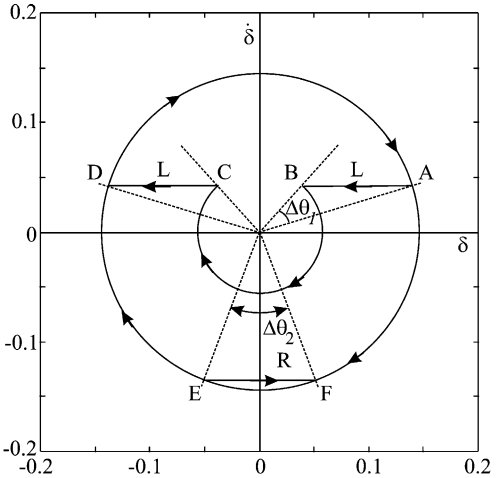

Fig. 6. Phase portrait for $\phi = 0.76$, $\mu = 3 \times 10^{-5}$, $K = 0.1$ showing an LLR mode with $\Omega = 2/3$.

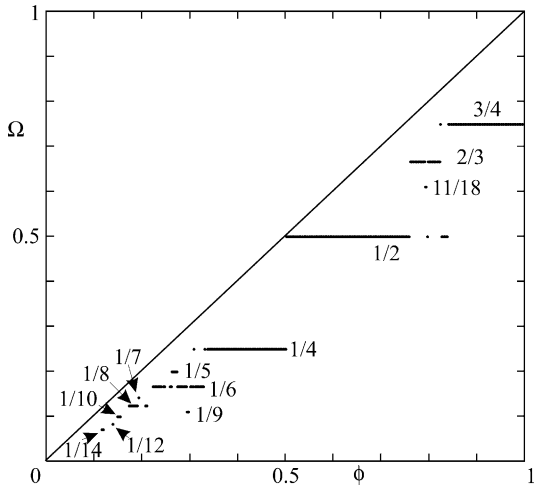

Fig. 7. Locking as a function of ϕ, for $\mu = 1 \times 10^{-2}$, $K = 0.1$.

5. Dependence on bubble period

The oscillator has been investigated for a fixed kick strength of $K = 0.1$ and fixed damping parameter $\mu = 1 \times 10^{-2}$. The period number ϕ is varied from 0.1 to 1.0 in steps of 0.002. The initial conditions of the oscillator are $\delta(0) = 0$ and $\dot{\delta}(0) = 0$. For each choice of parameters, first 1×10^6 bubbles are released (this number holds for all results presented here, unless mentioned otherwise). After that, another 20 000 bubbles are released and from the sequence {L, R} the smallest periodic part is obtained. As can be seen in Fig. 7, the rotation number is locked at low integer ratios, including $0/1$ that is found for several small values of ϕ. Note that the rotation number is not a monotonous number of ϕ. The plot shows a stair case which has some similarities with the well-known devil's staircase. However, here the steps of the staircase do not always climb up, but also sometimes go down.

If the friction parameter μ is decreased, the number of possible ratios for the rotation number increases. See Fig. 8 for example with $\mu = 1 \times 10^{-5}$. It is clear that in general at lower friction, the rotation number can stay

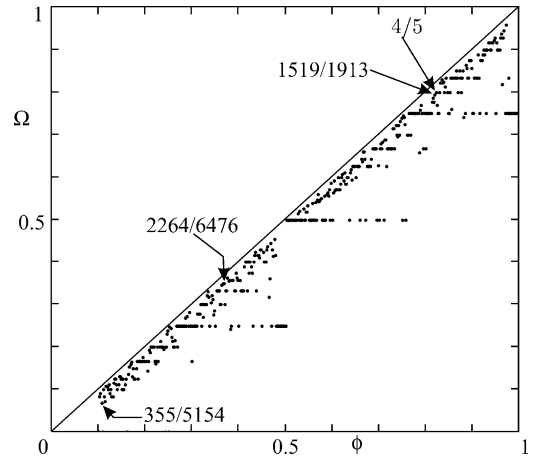

Fig. 8. Locking as a function of ϕ, for $\mu = 1 \times 10^{-5}$, $K = 0.1$.

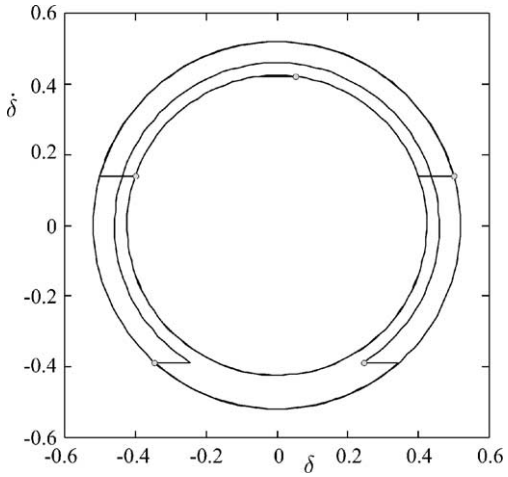

Fig. 9. Trajectory in phase space for $\phi = 0.822$, for $\mu = 1 \times 10^{-5}$, $K = 0.1$. The circles mark the positions at which the U-tube is kicked.

much closer to the period number. The staircase is broken up into many small steps. Only the steps '1/4', '1/2' and '3/4' can still be seen easily. In the figure a few data points are marked for which the rotation number is a ratio of large integers. These data points are distributed over the entire range of ϕ values. Furthermore, the rotation number can change quickly from a ratio of large integers, indicating a complex trajectory in phase space, to a simple one: see the two neighboring points $\phi = 0.82 \rightarrow \Omega = 1519/1913$ and $\phi = 0.822 \rightarrow \Omega = 4/5$. In between these two ϕ values several other ratios are found, seemingly without any order. The difference in behavior of the oscillator for these two values of ϕ is shown in the Figs. 9 and 10. The latter shows a Poincaré plot for the times just before the oscillator is kicked. The former shows both the trajectory in phase space as well as the Poincaré plot. The trajectory for $\phi = 0.822$ is simple and consists of only three parts of circles (apart form the very small damping). Here the trajectory is clearly 'quantized'. Only the sequence LLLRR is found. For $\phi = 0.82$ the trajectory consists of many different parts of circles, with diameters ranging from almost 0 to 1.12. The position in phase space of the oscillator

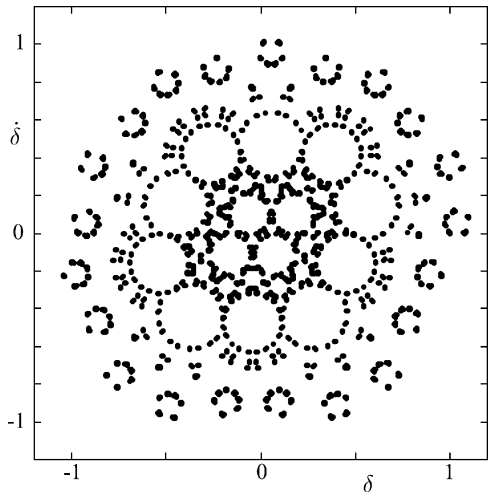

Fig. 10. Poincaré plot for $\phi = 0.82$, for $\mu = 1 \times 10^{-5}$, $K = 0.1$.

moves inward and outward several times before the trajectory repeats itself. The sequence is built of elementary blocks LR, LLR, LLRR, LLRRR, LLLRR, LLLRRR with the block of lengths 4 and 5 dominating in number. Note that increasing the initial number of kicks from 10^6 to 10^8 does not change the $\phi = 0.82$ case, the mode is still 1519/1913.

The pattern in Fig. 10 shows resemblance with the overflow oscillations reported for (lossless, second-order) digital filters (see e.g. [2,4]). For these systems the nonlinearity comes from the normalization of the signals to $[-1, 1)$. The overflow manifests itself as (discrete) 'kicks' in one of the variables of a strength sampled from the ternary $\{-2, 0, 2\}$. As mentioned in [4] the effect of damping on the overflow oscillations is that there is a progressive disappearance of long period oscillations. This is quite similar to what is observed in the damped kicked harmonic oscillator described here. For large damping, the overflow oscillation attracts to the fixed point at the origin and the period-2 limit cycle associated with $s = \{-2, +2\}$. Similarly, the damped kicked harmonic oscillator attracts to low period periodic orbits for large friction. A difference is, that in the case of the kicked oscillator the origin (in phase space) is not a fixed point as the kicks will, for positions close to the origin (i.e. $|\delta| < K/2$, see Fig. 2), always add extra energy to the system and kick it out of the origin for any value of the damping.

When the friction parameter μ is lowered further, the number of steps of the staircase increases further. Some of the trajectories have a very long sequence, like $\phi = 0.88$ and $\mu = 1 \times 10^{-8}$. The corresponding sequence is 14 718/76 000. For the case $\phi = 0.76$ and $\mu = 1 \times 10^{-8}$ no repetition could be found, i.e. the sequence is longer than 10^6 injected bubbles which are injected after the initial 10^6 bubbles that are used to start up the motion. The Poincaré plot for this situation is given in Fig. 11.

The Poincaré plot clearly shows, that the trajectory in phase space seems to be restricted to a finite value of the energy: a value of 0.8 for both δ and $\dot{\delta}$ is about the maximum. The positions at which the oscillator is kicked do not cover the enter range of values allowed by the energy. Instead a well defined pattern is formed, that leaves internally regions that are not part of the set of allowed kick-positions. This figure does not change noticeably when lowering the friction parameter to 0. However, if the initial number of bubbles injected is increased to 10^7, a 3/10 mode is found. The corresponding Poincaré plot is shown in Fig. 12. The figure shows that the trajectory is still more complicated than the simplest possible 3/10 mode. If the periodic points are calculated from Eq. (16) using a $s^k = \{-1, -1, 1, -1, -1, 1, 1, -1, 1, 1\}$, they are located inside each of the groups of five dots in Fig. 12. No

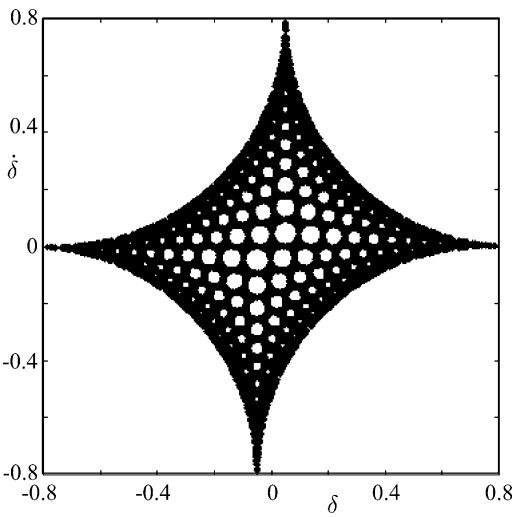

Fig. 11. Poincaré plot for $\phi = 0.76$, for $\mu = 1 \times 10^{-8}$, $K = 0.1$ after injecting 10^6 initial bubbles. The number of points plotted is 2×10^5.

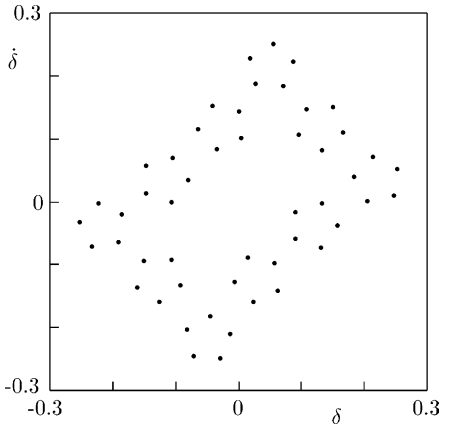

Fig. 12. Poincaré plot for $\phi = 0.76$, for $\mu = 1 \times 10^{-8}$, $K = 0.1$ after injecting 10^7 initial bubbles. The number of points plotted is 2×10^3.

sequence s^k has been found that generates the points in the Poincaré plot. This suggests that the system has not reached a steady state, i.e. it still is 'converging' to the simple 3/10 periodic orbit. Increasing the number of initial bubbles to 10^9 does not change the Poincaré plot of Fig. 12. Most likely, the 16-bit accuracy used is insufficient to see the further relaxation towards the steady state.

6. Dependence on friction parameter

In the previous section the bubbles injection time was varied. Here we will concentrate on variation of the friction in the system at a fixed value of $\phi = 0.76$ and a kick strength of $K = 0.1$. μ is varied from 1×10^{-2} to 1×10^{-8} in 2000 steps, logarithmically spaced over all values. Again, the initial conditions of the oscillator are $\delta(0) = 0$ and $\dot{\delta}(0) = 0$. Fig. 13 shows that at higher friction, the system locks on ratios of small integers. The trajectory in phase

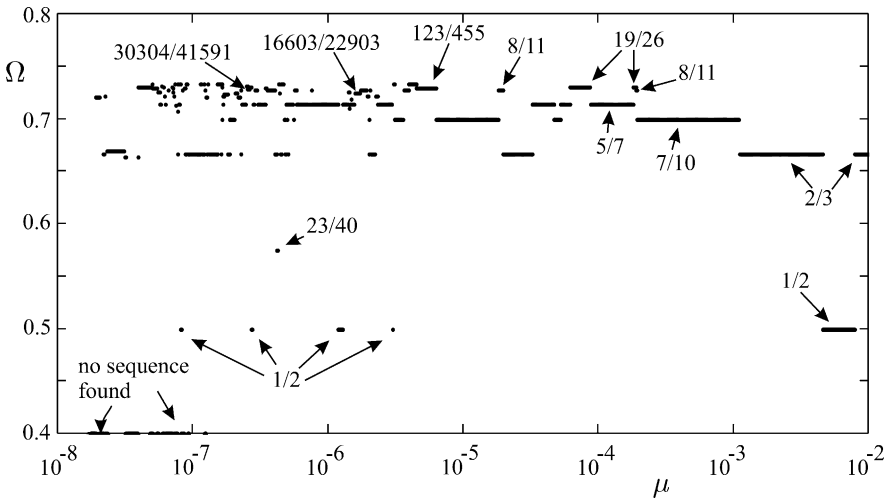

Fig. 13. Dependence of Ω on μ for $\phi = 0.76$, $K = 0.1$. The points with a value of 0.4 represents values of μ for which no sequence was found.

space is then 'simple', consisting of only a few different circles. As the friction gets smaller, more different rotation numbers are found, some being the ratio of two large integers. The corresponding trajectories will be complicated, with many 'quantized levels'. However, small changes in the friction parameter may cause the oscillator to go back to a simple trajectory at a rotation number of low integers. For each value of the friction parameter a repetition sequence of up to 1×10^5 kicks has been searched. Starting from $\mu = 1.2316860 \times 10^{-7}$ points appear in Fig. 13 for which the sequence is longer than 1×10^5 kicks. The first one has been searched for 2×10^6 kicks, but no repetition of a sequence was found. In the figure, these points have been put artificially at a value of 0.4 for the rotation number (that value is not possible as the period number is larger than 0.5). It might be that the repetition length is simply longer than the investigated one, but it could also mean that a steady state has not been reached similar to the case discussed above.

Surprisingly, at small values of the friction parameter, $\mu = 8.0816493 \times 10^{-8}$, still a rotation number of 1/2 is found. The oscillator is still kicked 1×10^6 bubbles before the trajectory is inspected. For μ values bigger than 1.1872×10^{-6} the $\Omega = 1/2$ trajectory is simple, see Fig. 14. The two points where the oscillator is kicked are marked by the gray circles. These points can be calculated directly from Eq. (16). The coordinates $\{\delta, \dot{\delta}\}$ of the kicks are $\{0.0500, 0.04708\}$ and $\{-0.0500, -0.0470\}$. The important point is that there are only two points were the system gets kicked.

This is no longer true for the 1/2 modes at lower values of μ. The next $1/2$ mode is found at 2.7447323×10^{-7}. The trajectory in phase space is much more complicated than the one shown in Fig. 14. The two positions were the oscillator is kicked seemed to be 'opened' and form a discrete set that circles around the original positions. This obviously also means that the trajectory in phase space consists of much more discrete circles. It is as if the original simple trajectory is opened showing a fine structure. Furthermore, the circles in this 'fine structure' have a 'hyper fine structure', i.e. they consist of two or three circles with only a small difference in radius (thus in energy of the oscillator). Both the trajectory and the Poincaré plot of the positions at the kicks are shown in Fig. 15. The number of bubbles injected before recording the trajectory is 1×10^6, like in all previous cases. If this number is increased, the dots contract towards the gray, central dots in Fig. 15 (right). When 1×10^7 bubbles kick the oscillator before the trajectory is recorded, the radius of the circle describing the kick positions is smaller than 0.005, whereas in Fig. 15 (right) it is bigger than 0.05. Eventually, for still much larger number of kicking bubbles, the system will find the stable trajectory with only two kicking positions. This low value of the friction parameter slows down the

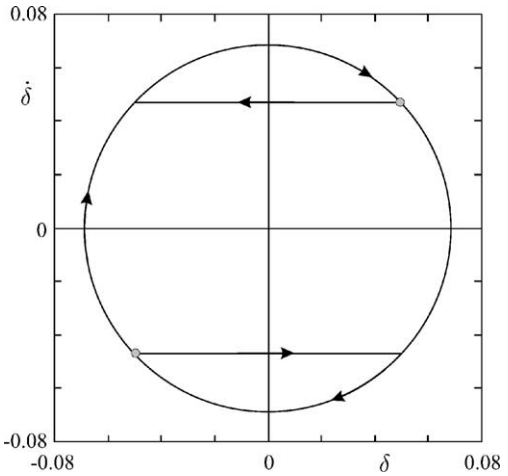

Fig. 14. Trajectory in phase space for $\mu = 1.1871347 \times 10^{-6}$, $\phi = 0.76$, $K = 0.1$.

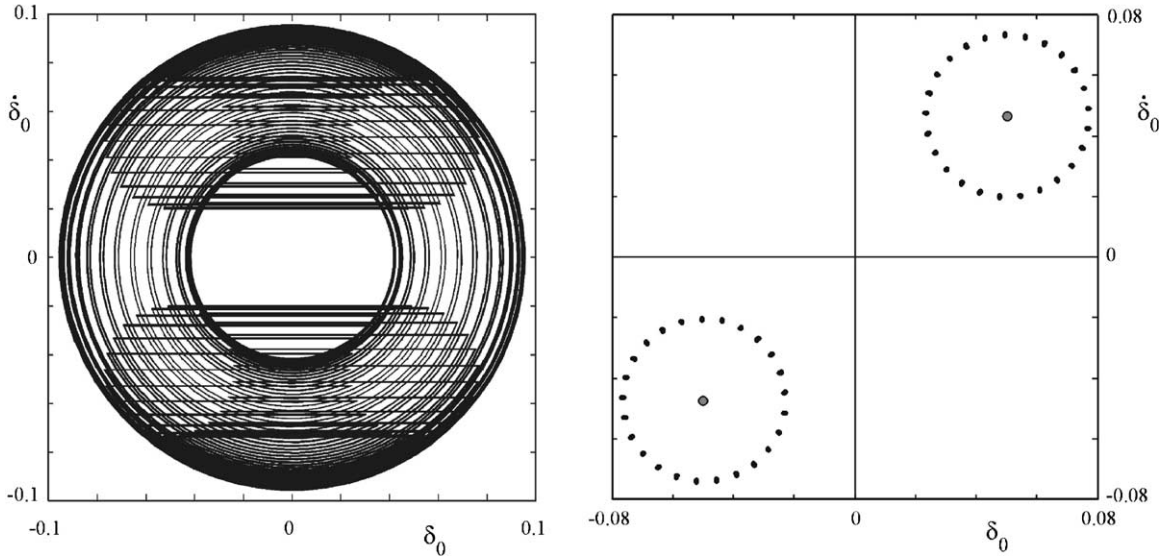

Fig. 15. $\mu = 2.7447323 \times 10^{-7}$, $\phi = 0.76$, $K = 0.1$: (left) trajectory in phase space, (right) Poincaré plot of kick positions. Both figures are the result of 20,000 kicks. Note that the two gray circles at $\{0.5, 0.5\}$ and $\{-0.5, -0.5\}$ are from the $1/2$ mode at higher values of the friction parameter.

relaxation to the final state tremendously, but in contrast to some of the examples discussed above the system clearly shows the relaxation towards the steady state.

From the above it is concluded that small changes in the friction parameter (or the period number) change the relaxation time of the system towards the steady state by orders of magnitude.

7. Initial conditions

In all the above, the U-tube was initially in its equilibrium position, i.e. $\delta_0 = 0$ and $\dot{\delta}_0 = 0$, when the oscillator was kicked for the first time. However, the locking of the oscillator is a function of the initial conditions. An example of this is shown in Fig. 16 for $\phi = 0.76$, $K = 0.001$ and $\mu = 4.17 \times 10^{-3}$. The initial conditions are varied from $\{-0.2, 0.2\}$ in steps of 0.001 for δ_0 as well as for $\dot{\delta}_0$. As can be seen, for most of the initial conditions the oscillator locks at mode $3/4$, i.e. close to $\phi = 0.76$. However, four 'arms' spiral away from the origin. In these arms several modes are found: $1/2$, $2/3$, $5/7$, $7/10$, $13/18$. The figure is symmetric. Furthermore, kinks in the arms when crossing the δ-axis are observed.

A zoom in the central region is shown in Fig. 17. The step size is now 1×10^{-4}. It shows that the dependence on the initial conditions is sensitive to small changes. The region around the origin is seen to be formed by locking modes $1/2$ and $2/3$ only. In Fig. 18 this region is further enlarged using a step size of 2×10^{-5}, confirming the previous observation. At this scale, still a sensitive dependence of the locking mode on the initial conditions is observed close to the origin. In [17] the influence of initial conditions on the trajectories in phase space is discussed for a damped harmonic oscillator kicked via wave packages. At relatively weak damping also here sensitivity to initial conditions is found. Furthermore, it was shown that at sufficiently low damping stationary points other than the origin are still present. Depending on the initial conditions the trajectory in phase space is attracted to different stationary points. The same holds for the present kicked oscillator.

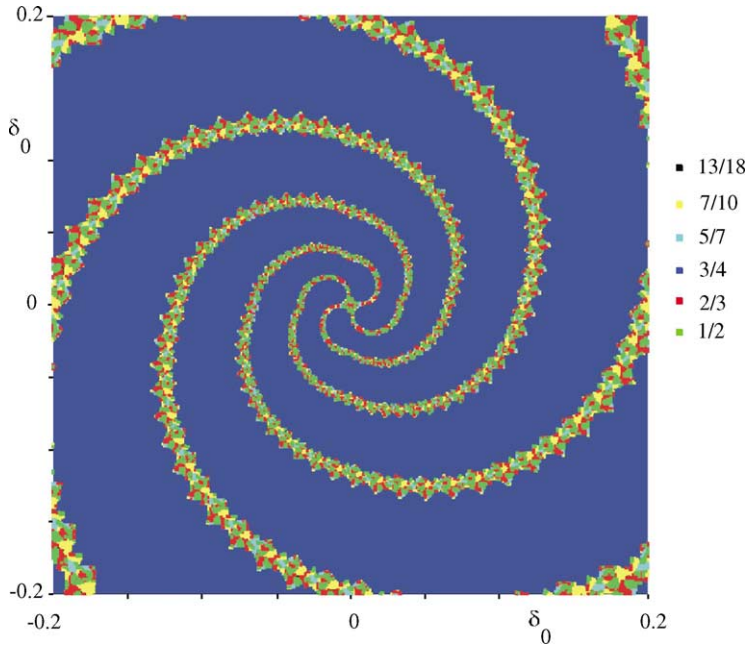

Fig. 16. Initial condition plot: $\mu = 4.17 \times 10^{-3}$, $\phi = 0.76$, $K = 0.001$.

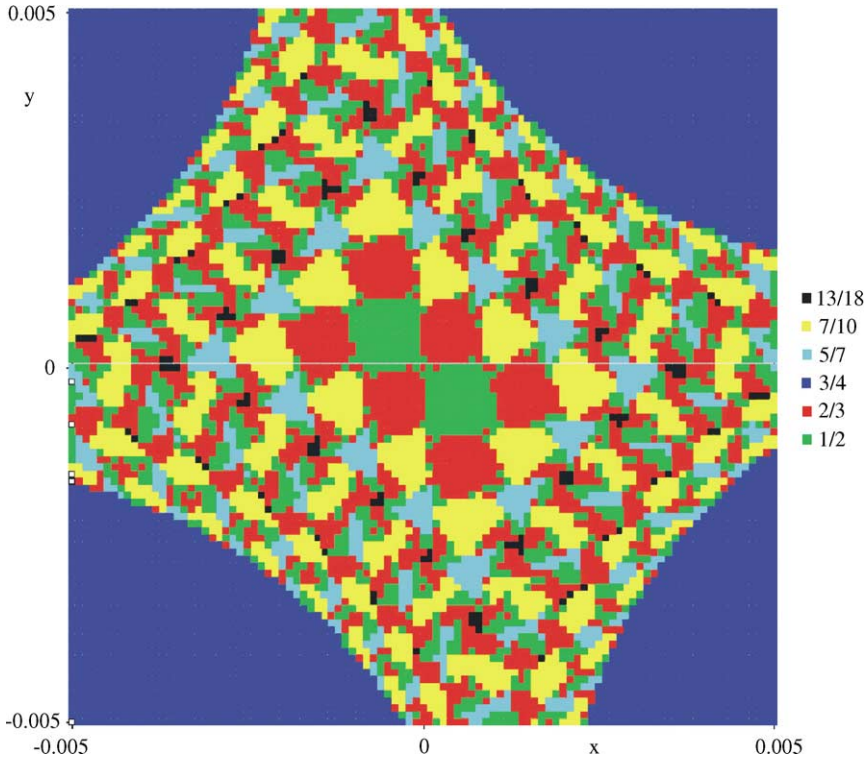

Fig. 17. Initial condition plot: $\mu = 4.17 \times 10^{-3}$, $\phi = 0.76$, $K = 0.001$.

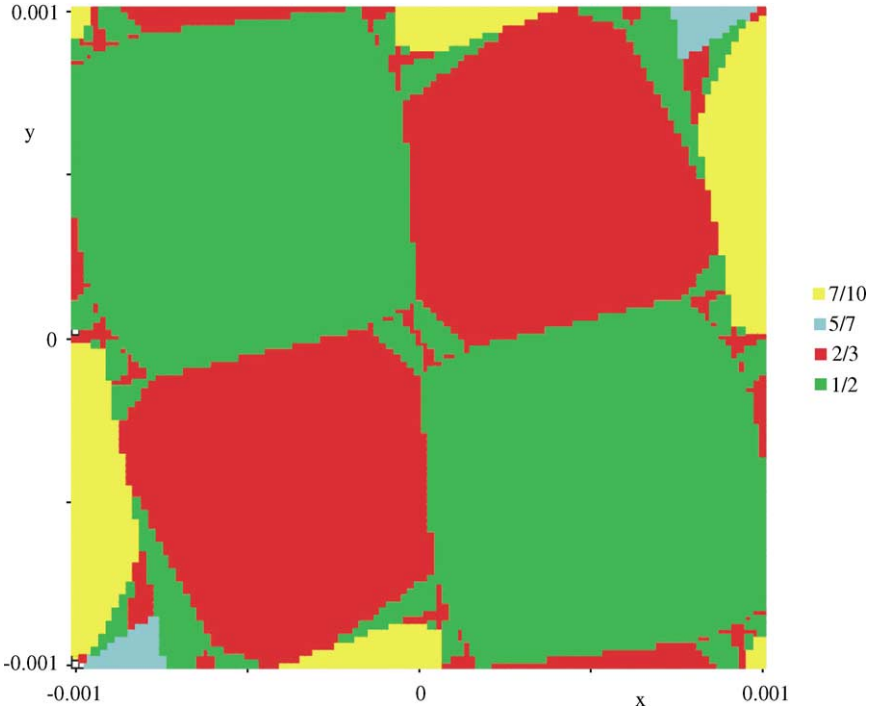

Fig. 18. Initial condition plot: $\mu = 4.17 \times 10^{-3}$, $\phi = 0.76$, $K = 0.001$.

8. Concluding remarks

In the present paper we investigate a damped oscillator kicked at a fixed frequency by a kick of fixed strength but a sign determined solely by the sign of the velocity of the oscillator. The system represents a simple U-tube filled with water and kicked by bubbles that enter the U-tube at the bottom. The stable orbits can be predicted via a simple analytical expression that describes the position of the (stable) points in phase space were the oscillator is kicked. However, the calculation requires the input of the sign of the kicks which cannot be predicted before hand, yet. The possible modes of the oscillator, expressed as a sequence of the signs of the kicks follows the rules of the Farey tree. For relatively high values of the friction parameter, the modes are formed by the ratio of small integers and the modes are in the top of the tree. For lower friction values, modes deeper in the tree are found, but it is not clear whether or not these modes are actually stable or that the required relaxation time is much longer.

It was found that the oscillator is not only sensitive to small changes in the period number, but also to small changes in the friction parameter. Finally, it is observed that the final mode of the oscillator is influenced by the initial position of the oscillator in phase space. For most of the initial conditions investigated at a fixed period number, friction and kick strength, the same behavior is found. However, four arms spiral away from the origin in the initial conditions plane for which the modes are different. In the present study, the time required for reaching the steady state is not investigated. This will require more research.

Acknowledgements

The authors like to thank Henk Bruin (University of Groningen, The Netherlands) for drawing our attention to piecewise isometries and circle mappings as well as for the stimulating discussions.

References

[1] V. Afanasiev, A. Chernikov, R. Sagdeev, G. Zaslavsky, The width of the stochastic web and particles diffusing along the web, Physica Lett. A 144 (1990) 229–236.
[2] P. Ashwin, W. Chambers, G. Petkov, Lossless digital filter overflow oscillations: approximation of invariant fractals, Int. J. Bifurcat. Chaos 11 (1997) 2603–2610.
[3] A. Chernikov, R. Sagdeev, G. Zaslavsky, Stochastic webs, Physica D 33 (1988) 65–76.
[4] A. Davies, Nonlinear oscillations and chaos from digital filter overflow, Phil. Trans. R. Soc. Lond. A 353 (1995) 85–99.
[5] S. Gardiner, J. Cirac, P. Zoller, Quantum chaos in an ion trap: the delta-kicked harmonic oscillator, Phys. Rev. Lett. 79 (1997) 4790–4793.
[6] B. Klappauf, W. Osaky, D. Steck, M. Raizen, Quantum chaos with cesium atoms: pushing the boundaries, Physica D 131 (1999) 78–89.
[7] A. Lichtenberg, B. Wood, Diffusion through a stochastic web, Phys. Rev. A 39 (1989) 2153–2159.
[8] R.F. Mudde, J.S. Groen, H.E.A. Van Den Akker, Liquid velocity field in a bubble column: LDA experiments, Chem. Eng. Sci. 52 (1997) 4217–4224.
[9] R.F. Mudde, D.J. Lee, J. Reese, L.-S. Fan, The role of coherent structures on the Reynolds stresses in a two-dimensional bubble column, AIChE J. 43 (4) (1997) 913–926.
[10] R.F. Mudde, T. Saito, Hydrodynamical similarities between bubble column and bubbly pipeflow, J. Fluid Mech. 437 (2001) 203–228.
[11] L. Reichl, The Transition to Chaos, Springer, Berlin, 1987.
[12] A. Scott, C. Holmes, G. Milburn, Quantum and classical chaos for a single trapped ion, Phys. Rev. A 61 (2000) 3401–3405.
[13] A. Scott, C. Holmes, G. Milburn, Hamiltonian mappings and circle packing phase spaces, Physica D 155 (2001) 34–50.
[14] A. Scott, G. Milburn, Periodic orbit quantization of a hamiltonian map on the sphere, J. Phys. A 34 (2001) 7541–7562.
[15] S. Tanabe, S. Watanabe, N. Stao, M. Matsuzawa, S. Yoshida, C. Reinhold, J. Burgdörfer, Siegert-pseudostate representation of quantal time evolution: a harmonic oscillator kicked by periodic pulses, Phys. Rev. A 63 (2001).
[16] R.W. Van Den Berg, Interplaying time scales in two-phase flows, Ph.D. Thesis, Delft University of Technology, The Netherlands, 1996.
[17] A. Vasil'ev, G. Zaslavskiĭ, M. Natenzon, A. Neĭstadt, B. Petrovichev, R. Sagdeev, A. Chernikov, Attractors and stochastic attractors of motion in a magnetic field, Sov. Phys. JETP 67 (1988) 2053–2062.
[18] G. Zaslavskiĭ, M. Zakharov, R. Sagdeev, D. Usikov, A. Chernikov, Stochastic web and diffusion of particles in a magnetic field, Sov. Phys. JETP 64 (1986) 294–303.